Quasiclassical theory of the dynamical ExE Jahn-Teller effect including spin-orbit interaction

Leonid V Poluyanov, Sabyashachi Mishra, Wolfgang Domcke

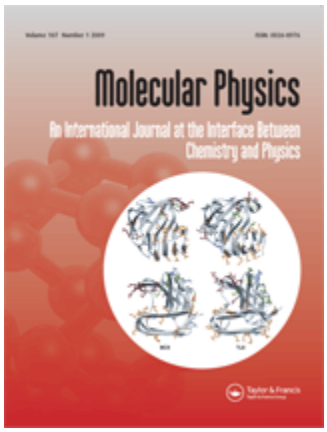

Quasiclassical theory of the dynamical ExE Jahn-Teller effect including spin-orbit interaction

Journal:	*Molecular Physics*
Manuscript ID:	TMPH-2006-0070.R1
Manuscript Type:	Full Paper
Date Submitted by the Author:	28-Nov-2006
Complete List of Authors:	Poluyanov, Leonid; Academy of Sciences, Institute of Chemical Physics Mishra, Sabyashachi; Technical University of Munich, Department of Chemistry Domcke, Wolfgang; Technical University of Munich, Department of Chemistry
Keywords:	Jahn-Teller effect, Spin-orbit interaction, quasiclassical analysis , Landau-Zener case
Note: The following files were submitted by the author for peer review, but cannot be converted to PDF. You must view these files (e.g. movies) online.	
QC-JTSO.tex	

Quasiclassical theory of the dynamical $E \times E$ Jahn-Teller effect including spin-orbit interaction

Leonid V. Poluyanov,[1] Sabyashachi Mishra,[2,*] and Wolfgang Domcke[2]

[1]*Institute of Chemical Physics,*

Academy of Sciences, Chernogolovka, Moscow 142432, Russia

[2]*Department of Chemistry,*

Technical University of Munich, D-85747 Garching, Germany

(Dated: November 28, 2006)

Abstract

The dynamical Jahn-Teller effect including spin-orbit coupling is considered in the coordinate and momentum representations of the nuclear motion. The momentum representation is used for the asymptotical solution of the dynamical equations in the quasiclassical Landau-Zener parametric limiting case. Vibronic energy levels of the $E \times E$ Jahn-Teller effect with spin-orbit coupling are calculated from the quasiclassical secular equation. They are compared with numerically exact energy levels obtained by the diagonalization of the Hamiltonian matrix in a harmonic oscillator basis. The comparison reveals reasonable accuracy of the quasiclassical approximation for a wide range of quantum numbers and system parameters. The quasiclassical analysis provides insight into the nature of the nonadiabatic dynamics of $E \times E$ Jahn-Teller systems with spin-orbit coupling.

1. INTRODUCTION

In this work, we develop an analytical description of the quantum dynamics of the $E \times E$ Jahn-Teller (JT) effect with inclusion of the spin-orbit (SO) interaction. The SO interaction is of relativistic origin and causes an energy splitting 2Δ of the potential-energy surfaces (PES) at the symmetrical configuration of the system. The existence of the SO splitting has a significant impact on the dynamics of the JT problem. Unlike in the nonrelativistic case ($\Delta = 0$), there are three nonadiabatic transition centers (where nonadiabatic coupling terms become singular). In addition, a radial nonadiabatic coupling term appears in the dynamical equations. The radial adiabatic potentials contain several new terms of SO origin. In this work, the main attention is paid to the interplay of the SO splitting and the linear vibronic coupling, both of which are responsible for nonadiabatic transitions in the system.

The Hamiltonian of the $E \times E$ JT effect with SO coupling was proposed in previous works, see Ref. 1–3 and references therein. In methodological sense, the present work is close to the quasiclassical (QC) analysis of the nonrelativistic $E \times E$ JT problem by Osherov and Voronin[4]. The history of studies of the energy-level spectrum of the $E \times E$ JT effect without SO coupling includes, among many others, the works of Teller and Jahn[5,6], Wigner and Neumann[7,8], Longuet-Higgins[9], Osherov and Voronin[4,10], and Judd[11,12]. Many results and useful references can be found in the books of Bersuker[13], Nikitin[14], and Domcke, Yarkony, and Köppel[15]. The literature on the JT effect including SO coupling is less extensive. Even the linear approximation (in the degenerate vibrational mode) for the JT-SO Hamiltonian seems to be a rich problem. We consider here the linear approximation in order to deduce the dynamical equations in the momentum representation,

define transformations between the coordinate and momentum representations and derive the local nonadiabatic S-matrix. This S-matrix plays a central role for the formulation of the quantization condition for the vibronic energy levels of the linear $E \times E$ JT Hamiltonian which includes an isotropic quadratic term. The second-order JT coupling is not taken into account here. As is well known, this simplification leads to rotationally symmetrical PES and allows us to perform a separation of the radial and angular variables in the vibronic Schrödinger equation.

Our calculations are of asymptotical character. Several special mathematical techniques (such as the matched-asymptotic-expansion method, the ordered-exponential-operator method, and the stationary-phase method) play an essential role in the analysis. We derive a transcendental secular equation for the vibronic energy levels in terms of transparent QC and nonadiabatic concepts. This systematic approach is rather general and can therefore be applied to a variety of vibronic-coupling problems.

In order to verify the validity and accuracy of the asymptotical methodology, we compare with the results of numerically exact calculations of vibronic energy levels of the JT-SO Hamiltonian. Comparing the results obtained by this two completely different methods, we find reasonably good agreement and arrive at a transparent interpretation of the nonadiabatic effects in the JT-SO problem.

2. THE DYNAMICAL EQUATIONS IN THE COORDINATE REPRESENTATION

Following Koizumi and Sugano[1], Schön and Köppel[2] and others, we consider the linear $E \times E$ JT-Hamiltonian with SO coupling

$$\hat{H}_{\mathrm{JT}} = -\frac{\hbar^2}{2M}\left(\frac{\partial^2}{\partial x^2}+\frac{\partial^2}{\partial y^2}\right) + \begin{pmatrix} \Delta & F(x+iy) \\ F(x-iy) & -\Delta \end{pmatrix} + \frac{M\omega^2}{2}(x^2+y^2), \qquad (1)$$

where x and y are the two components of the degenerate normal coordinate of E symmetry, F is the linear JT coupling constant, 2Δ is the SO splitting of the degenerate electronic state in the symmetrical configuration, and M is the mass parameter associated with the vibrational mode. In the following, we will consider the linear $E \times E$ JT effect in the absence of a harmonic restoring potential (the last term on the right-hand side of Eq. (1)). The latter will be introduced in a later stage of the analysis.

In polar coordinates (ρ, φ),

$$x \pm iy = \rho e^{\pm i\varphi}$$

we have

$$\hat{H} = \hat{H}_{\rm JT} - \frac{M\omega^2}{2}\rho^2 = -\frac{\hbar^2}{2M}\left(\frac{\partial^2}{\partial\rho^2} + \frac{1}{\rho}\frac{\partial}{\partial\rho} + \frac{1}{\rho^2}\frac{\partial^2}{\partial\varphi^2}\right) + \begin{pmatrix} \Delta & \rho F e^{i\varphi} \\ \rho F e^{-i\varphi} & -\Delta \end{pmatrix}. \quad (2)$$

The Hamiltonian $\hat{H}$ commutes with the symmetry operator

$$\hat{J}_z = -i\frac{\partial}{\partial\varphi} - \hat{\sigma}_z \quad (3)$$

where $\hat{\sigma}_z$ is one of the Pauli matrices.

The common eigenfunctions of $\hat{H}$ and $\hat{J}_z$ can be written as,

$$\vec{\psi}_m(\rho,\varphi) = \frac{1}{\sqrt{\rho}}\begin{pmatrix} f_m^{(1)}(\rho)\ e^{i(m+1/2)\varphi} \\ f_m^{(2)}(\rho)\ e^{i(m-1/2)\varphi} \end{pmatrix} \quad (4)$$

where $m = \pm 1/2, \pm 3/2 \cdots$ is the half integer vibronic angular momentum quantum number.

The coupled equations for the radial functions $f_m^{(1)}(\rho)$ and $f_m^{(2)}(\rho)$ can be written as

$$\hat{H}_m \vec{f}_m(\rho) = E_m \vec{f}_m(\rho),$$

$$\vec{f}_m(\rho) = \vec{f}_m^{(1)}(\rho)\vec{e}_1 + \vec{f}_m^{(2)}(\rho)\vec{e}_2,$$

$$\hat{H}_m = -\frac{\hbar^2}{2M}\frac{\mathrm{d}^2}{\mathrm{d}\rho^2} + \frac{m^2\hbar^2}{2M\rho^2} + 2\left(\Delta + \frac{m\hbar^2}{2M\rho^2}\right)\hat{\sigma}_z + 2\rho F\hat{\sigma}_x \tag{5}$$

where $\hat{\sigma}_x$ and $\hat{\sigma}_z$ are Pauli matrices, $\vec{e}_1 = \begin{pmatrix} 1 \\ 0 \end{pmatrix}$ and $\vec{e}_2 = \begin{pmatrix} 0 \\ 1 \end{pmatrix}$.

There exists a discrete symmetry operator $\hat{S}_m$ which commutes with the radial Hamiltonian $\hat{H}_m$

$$\hat{S}_m = (\Delta \to -\Delta)(m \to -m)\hat{\sigma}_x. \tag{6}$$

This property of $\hat{H}_m$ guarantees that

$$E_m(\Delta) = E_{-m}(-\Delta). \tag{7}$$

Let us consider the adiabatic representation of the Hamiltonian (2), defined as[1–3]:

$$\hat{H}_a\vec{\psi}_a = E\vec{\psi}_a$$

$$\hat{H}_a = \hat{W}^\dagger\hat{H}\hat{W}; \qquad \vec{\psi}_a = \hat{W}^\dagger\vec{\psi} \tag{8}$$

where

$$\hat{W} = \begin{pmatrix} \cos\theta\ e^{i\varphi/2} & \sin\theta\ e^{i\varphi/2} \\ -\sin\theta\ e^{-i\varphi/2} & \cos\theta\ e^{-i\varphi/2} \end{pmatrix} \tag{9}$$

$$\begin{aligned} \cos\theta &= \frac{\rho F}{\sqrt{(U-\Delta)^2 + \rho^2F^2}} > 0 \\ \sin\theta &= -\frac{U-\Delta}{\sqrt{(U-\Delta)^2 + \rho^2F^2}} < 0 \\ U &= \sqrt{\rho^2F^2 + \Delta^2}. \end{aligned} \tag{10}$$

The unitary transformation $\hat{W}$ is chosen to diagonalize the potential-energy part of the Hamiltonian (2). Somewhat lengthy but straightforward calculations give the Hamiltonian in the adiabatic

representation,

$$\hat{H}_a = -\frac{\hbar^2}{2M}\left[\frac{\partial^2}{\partial\rho^2}+\frac{1}{\rho}\frac{\partial}{\partial\rho}+\frac{1}{\rho^2}\frac{\partial^2}{\partial\varphi^2}-\theta'^2-\frac{1}{4\rho^2}+ 4i\theta'\hat{\sigma}_y\frac{\partial}{\partial\rho}+\frac{2i}{\rho^2}\left(\cos 2\theta\cdot\hat{\sigma}_z+\sin 2\theta\cdot\hat{\sigma}_x\right)\frac{\partial}{\partial\varphi}+ 2i\theta''\hat{\sigma}_y+\frac{2i}{\rho}\theta'\hat{\sigma}_y\right]+2U\hat{\sigma}_z \quad (11)$$

where

$$\theta' = -\frac{\Delta F}{U^2}<0$$
$$\theta'' = \frac{\rho\Delta F^3}{U^4}\geq 0. \quad (12)$$

The adiabatic PES are

$$U_\pm(\rho)=\pm U=\pm\sqrt{\rho^2F^2+\Delta^2}, \quad (13)$$

forming a rotationally symmetric double hyperboloid. The SO splitting Δ gives rise to the existence of an additional radial nonadiabatic coupling term in Eq. (11)

$$(2i\hbar^2\Delta F/MU^2)\hat{\sigma}_y\frac{\partial}{\partial\rho}.$$

The Hamiltonian $\hat{H}_a$ is characterized by the symmetry operator

$$\hat{l}_z=-i\frac{\partial}{\partial\varphi}. \quad (14)$$

The common eigenfunctions of $\hat{H}_a$ and $\hat{l}_z$,

$$\hat{H}_a\vec{\psi}_a^{(m)} = E_m\vec{\psi}_a^{(m)}(\rho,\varphi)$$
$$\hat{l}_z\vec{\psi}_a^{(m)} = m\vec{\psi}_a^{(m)}(\rho,\varphi) \quad (15)$$

have the form,

$$\vec{\psi}_a^{(m)}=\frac{1}{\sqrt{\rho}}\begin{pmatrix}\vec{\psi}_m^{(1)}(\rho)\\ \vec{\psi}_m^{(2)}(\rho)\end{pmatrix}e^{im\varphi}\quad m=\pm1/2,\pm3/2,\cdots \quad (16)$$

The coupled equations for the radial functions in the adiabatic representation can be written as:

$$\hat{H}_a^{(m)}\vec{\psi}_m^{(a)}(\rho) = E_m\vec{\psi}_m^{(a)}(\rho)$$

$$\vec{\psi}_m^{(a)}(\rho) = \vec{\psi}_m^{(1)}(\rho)\vec{e}_1 + \vec{\psi}_m^{(2)}(\rho)\vec{e}_2$$

$$\begin{aligned}\hat{H}_a^{(m)} &= -\frac{\hbar^2}{2M}\left[\frac{\mathrm{d}^2}{\mathrm{d}\rho^2} - \frac{m^2}{\rho^2} - \theta'^2 + 4i\theta'\hat{\sigma}_y\frac{\mathrm{d}}{\mathrm{d}\rho} - \right.\\ &\left.\frac{2m}{\rho^2}\left(\cos 2\theta\cdot\hat{\sigma}_z + \sin 2\theta\cdot\hat{\sigma}_x\right) + 2i\theta''\hat{\sigma}_y\right] + 2U\hat{\sigma}_z. \qquad (17)\end{aligned}$$

Equation (17) allows us to introduce effective adiabatic radial potentials:

$$U_\rho^{\pm} = \frac{\hbar^2}{2M}\left(\frac{m^2}{\rho^2} + \frac{\Delta^2F^2}{4U^4} \pm \frac{m\Delta}{\rho^2U}\right) \pm U, \qquad (18)$$

which are shown in Fig. 1.

There exists again a discrete symmetry operator $\hat{S}_a^{(m)}$ which commutes with $\hat{H}_a^m$

$$\hat{S}_a^{(m)} = (\Delta \to -\Delta)(m \to -m)\hat{\sigma}_z. \qquad (19)$$

Note, that both $\hat{H}_m$ and $\hat{H}_a^{(m)}$ are real and thus commute with the operator of complex conjugation.

3. THE DYNAMICAL EQUATIONS IN THE MOMENTUM REPRESENTATION

Following Voronin and Osherov[4], we deduce the dynamical equations in the momentum representation. We start from Eq. (1) and perform a two-dimensional Fourier transformation of the diabatic amplitude vector $\vec{\psi}(x,y)$:

$$\vec{\phi}(k_x,k_y) = \frac{1}{2\pi}\int\int_{-\infty}^{\infty}\vec{\psi}(x,y)e^{-ixk_x-iyk_y}\,\mathrm{d}x\,\mathrm{d}y, \qquad (20a)$$

$$\vec{\psi}(x,y) = \frac{1}{2\pi}\int\int_{-\infty}^{\infty}\vec{\phi}(k_x,k_y)e^{ixk_x+iyk_y}\,\mathrm{d}k_x\,\mathrm{d}k_y. \qquad (20b)$$

Below we shall suppose that $|\vec{\psi}| \to 0$ when $x^2+y^2 \to \infty$. This guarantees the convergence of the Fourier integral (20a).

The equation of motion in the momentum representation reads

$$\hat{\mathcal{H}}\vec{\phi}(k_x,k_y) = E\vec{\phi}(k_x,k_y) \tag{21}$$

where

$$\hat{\mathcal{H}} = \frac{\hbar^2(k_x^2+k_y^2)}{2M} + 2iF\hat{\sigma}_x\frac{\partial}{\partial k_x} - 2iF\hat{\sigma}_y\frac{\partial}{\partial k_y} + 2\Delta\hat{\sigma}_z \tag{22}$$

is the Hamiltonian in the diabatic momentum representation.

The symmetry properties of the operator $\hat{\mathcal{H}}$ are:

$$\begin{aligned}\left[\hat{\mathcal{H}},\hat{j}_z\right] &= 0\\ \left[\hat{\mathcal{H}},\hat{\tau}\right] &= 0\end{aligned} \tag{23}$$

where

$$\begin{aligned}\hat{j}_z &= i\left(k_y\frac{\partial}{\partial k_x} - k_x\frac{\partial}{\partial k_y}\right) - \hat{\sigma}_z\\ \hat{\tau} &= (k_x\rightarrow -k_x)(k_y\rightarrow -k_y)\hat{h.c.}\end{aligned} \tag{24}$$

and $\hat{h.c.}$ denotes the operator of Hermitian conjugation.

Let us introduce polar coordinates in momentum space:

$$k_x \pm ik_y = ke^{\pm i\alpha}.$$

The Hamiltonian $\hat{\mathcal{H}}$ and the symmetry operators then take the form:

$$\begin{aligned}\hat{\mathcal{H}} &= \frac{\hbar^2k^2}{2M} + 2iF(\hat{\sigma}_x\cos\alpha - \hat{\sigma}_y\sin\alpha)\frac{\partial}{\partial k}\\ &\quad -\frac{2iF}{k}(\hat{\sigma}_x\sin\alpha + \hat{\sigma}_y\cos\alpha)\frac{\partial}{\partial\alpha} + 2\Delta\hat{\sigma}_z\end{aligned} \tag{25}$$

$$\hat{j}_z = -i\frac{\partial}{\partial\alpha} - \hat{\sigma}_z \tag{26}$$

$$\hat{\tau} = (\alpha\rightarrow\alpha\pm\pi)\hat{h.c.}. \tag{27}$$

The common eigenfunctions of $\hat{\mathcal{H}}$ and $\hat{j}_z$ in polar coordinates read

$$\vec{\phi}_m(k,\alpha) = \begin{bmatrix} f_m^{(1)}(k)\ e^{i(m+1/2)\alpha} \\ f_m^{(2)}(k)\ e^{i(m-1/2)\alpha} \end{bmatrix} \tag{28}$$

and the coupled radial equations of motion are

$$\hat{\mathcal{H}}_m \vec{f}_m(k) = E_m \vec{f}_m(k) \tag{29a}$$

$$\vec{f}_m(k) = \vec{f}_m^{(1)}(k)\vec{e}_1 + \vec{f}_m^{(2)}(k)\vec{e}_2 \tag{29b}$$

$$\hat{\mathcal{H}}_m = \frac{\hbar^2 k^2}{2M} + 2iF\hat{\sigma}_x\left(\frac{1}{2k} + \frac{\mathrm{d}}{\mathrm{d}k}\right) + \frac{2mF}{k}\hat{\sigma}_y + 2\Delta\hat{\sigma}_z. \tag{29c}$$

It is convenient to transform Eqs. (29b) and (29c) such that the differential operator $\mathrm{d}/\mathrm{d}k$ appears in the diagonal. Introducing the new vector function

$$\vec{g}_m(k) = \sqrt{k}\hat{U}_f^{-1}\vec{f}_m(k) \tag{30}$$

where

$$\hat{U}_f = \hat{U}_f^{-1} = \frac{1}{\sqrt{2}}\begin{pmatrix} 1 & 1 \\ 1 & -1 \end{pmatrix},$$

we have:

$$\hat{H}^{(m)}\vec{g}_m(k) = E_m\vec{g}_m(k)$$

$$\vec{g}_m(k) = \vec{g}_m^{(1)}(k)\vec{e}_1 + \vec{g}_m^{(2)}(k)\vec{e}_2$$

$$\hat{H}^{(m)} = \frac{\hbar^2 k^2}{2M} + 2iF\hat{\sigma}_z\frac{\mathrm{d}}{\mathrm{d}k} - \frac{2mF}{k}\hat{\sigma}_y + 2\Delta\hat{\sigma}_x. \tag{31}$$

The Hamiltonian $\hat{H}^{(m)}$ commutes with the following discrete symmetry operator:

$$\hat{\tau}_m = (m \to -m)\hat{tr} \tag{32}$$

where $\hat{tr}$ is the operator of matrix transposition. The coupled radial equations (31) can be written in the following useful form:

$$iF\frac{\mathrm{d}\vec{g}_m}{\mathrm{d}k} = \begin{pmatrix} -\frac{\hbar^2k^2}{2M} + E_m & -\Delta - \frac{imF}{k} \\ \Delta - \frac{imF}{k} & \frac{\hbar^2k^2}{2M} - E_m \end{pmatrix} \vec{g}_m. \tag{33}$$

The dynamical equations (33) are characterized by an exact conservation law[4]:

$$I = |g_m^{(1)}(k)|^2 - |g_m^{(2)}(k)|^2 = \text{const}. \tag{34}$$

Let us define

$$\vec{g}_m(k) = \hat{U}(k)\vec{g}_{mo} \tag{35}$$

where $\vec{g}_{mo}$ is a constant vector and $\hat{U}(k)$ is 2×2 matrix,

$$\hat{U}(k) = \begin{pmatrix} u_{11}(k) & u_{12}(k) \\ u_{21}(k) & u_{22}(k) \end{pmatrix} \tag{36}$$

The matrix $\hat{U}(k)$ has to conserve the integral of motion I. The most general form of $\hat{U}$ is given by hyperbolic unitary matrices:

$$\hat{U} = \begin{pmatrix} \cosh\alpha\ e^{i\chi_{11}} & \sinh\alpha\ e^{i\chi_{11}+i\delta_0} \\ \sinh\alpha\ e^{i\chi_{22}-i\delta_0} & \cosh\alpha\ e^{i\chi_{22}} \end{pmatrix} \tag{37}$$

which contain one hyperbolic angle α $[-\infty < \alpha(k) < +\infty]$ and the three trigonometric angles $\chi_{11}, \chi_{22}, \delta_0$ $[-\pi \leq \chi_{11}(k), \chi_{22}(k), \delta_0(k) \leq +\pi]$. Of course, the determination of the functions $\alpha(k), \chi_{11}(k), \chi_{22}(k), \delta_0(k)$ is equivalent to the solution of Eq. (33). Note, that the columns of the matrix (37) are the fundamental solutions of Eq. (33).

Now we can perform the separation of variables in the two-dimensional Fourier integral transformations (20). As a result, we can directly connect the radial amplitudes (in coordinate and momentum representations, respectively) by an integral transformation. The substitution of (4)

and (28) into (20a) gives:

$$\begin{pmatrix} f_m^{(1)}(k) \\ f_m^{(2)}(k) \end{pmatrix} = \frac{1}{2\pi} \int_0^\infty \sqrt{\rho}\, \mathrm{d}\rho \int_{-\pi}^{\pi} \mathrm{d}\varphi \begin{pmatrix} f_m^{(1)}(\rho) e^{i(m+1/2)\varphi - ik\rho\cos\varphi} \\ f_m^{(2)}(\rho) e^{i(m-1/2)\varphi - ik\rho\cos\varphi} \end{pmatrix}. \tag{38}$$

The angular integrals on the right-hand side of Eq. (38) can be calculated with the use of the known integral representation of the Bessel functions[16]:

$$\frac{1}{2\pi} \int_{-\pi}^{\pi} e^{in\varphi - iz\cos\varphi}\, \mathrm{d}\varphi = e^{-in\pi/2} J_n(z). \tag{39}$$

We thus have

$$\vec{f}_m(k) = \int_0^\infty \hat{N}_d^{(m)}(k\rho) \vec{f}_m(\rho) \sqrt{\rho}\, \mathrm{d}\rho \tag{40}$$

where

$$\hat{N}_d^{(m)}(k\rho) = \begin{pmatrix} e^{-i(m+1/2)\pi/2} J_{m+1/2}(k\rho) & 0 \\ 0 & e^{-i(m-1/2)\pi/2} J_{m-1/2}(k\rho) \end{pmatrix}.$$

Taking into account Eqs. (4), (8), (9), (16), (28), and (30), we arrive at a connection of the ρ-dependent amplitudes $\vec{\psi}_m^{(a)}(\rho)$ in the adiabatic coordinate representation with the k-dependent amplitudes $\vec{g}_m(k)$ in the momentum representation:

$$\vec{g}_m(k) = \int_0^\infty \hat{N}_m(k,\rho) \vec{\psi}_m^{(a)}(\rho)\, \mathrm{d}\rho \tag{41}$$

where

$$\hat{N}_m(k,\rho) = \sqrt{\frac{k\rho}{2}} \begin{pmatrix} (-i)^{m+1/2} J_{m+1/2}(k\rho)\cos\theta(\rho) - & (-i)^{m+1/2} J_{m+1/2}(k\rho)\sin\theta(\rho) + \\ (-i)^{m-1/2} J_{m-1/2}(k\rho)\sin\theta(\rho) & (-i)^{m-1/2} J_{m-1/2}(k\rho)\cos\theta(\rho) \\ \\ (-i)^{m+1/2} J_{m+1/2}(k\rho)\cos\theta(\rho) + & (-i)^{m+1/2} J_{m+1/2}(k\rho)\sin\theta(\rho) - \\ (-i)^{m-1/2} J_{m-1/2}(k\rho)\sin\theta(\rho) & (-i)^{m-1/2} J_{m-1/2}(k\rho)\cos\theta(\rho) \end{pmatrix}.$$

Another useful relation is:

$$\vec{g}_m(k) = \int_0^\infty \hat{N}^{(m)}(k\rho) \vec{f}_m(\rho)\, \mathrm{d}\rho \tag{42}$$

where

$$\hat{N}^{(m)}(k\rho) = \sqrt{\frac{k\rho}{2}} \begin{pmatrix} (-i)^{m+1/2} J_{m+1/2}(k\rho) & (-i)^{m-1/2} J_{m-1/2}(k\rho) \\ (-i)^{m+1/2} J_{m+1/2}(k\rho) & -(-i)^{m-1/2} J_{m-1/2}(k\rho) \end{pmatrix}.$$

The inverse transformations are:

$$\vec{f}_m(\rho) = \sqrt{\rho} \int_0^\infty \hat{N}_d^{(m)*}(k\rho) \vec{f}_m(k) k \, \mathrm{d}k \tag{43a}$$

$$\vec{f}_m(\rho) = \int_0^\infty \hat{N}^{(m)\dagger}(k\rho) \vec{g}_m(k) \, \mathrm{d}k \tag{43b}$$

$$\vec{\psi}_m^{(a)}(\rho) = \int_0^\infty \hat{N}_m^\dagger(k,\rho) \vec{g}_m(k) \, \mathrm{d}k. \tag{43c}$$

If we can solve Eq. (33), then we can, using the inverse transformation (43), obtain $\vec{f}_m(\rho)$ or $\vec{\psi}_m^{(a)}$. The main advantage of the momentum representation is the reduction of the order of the dynamical differential equations from four (in the coordinate representation) to two (in the momentum representation). This feature essentially facilitates the solution of the dynamical equations.

4. DIMENSIONLESS FORM OF THE DYNAMICAL EQUATIONS IN THE LANDAU-ZENER LIMITING CASE

Let us introduce the dimensionless independent variable τ in Eq. (33):

$$\tau = \rho_* k; \qquad \rho_* = \hbar/p_0; \qquad p_0 = \sqrt{2ME}. \tag{44}$$

Equation (33) then takes the form:

$$i\frac{\mathrm{d}\vec{g}_m}{\mathrm{d}\tau} = \begin{pmatrix} \frac{E}{\rho_* F}(1-\tau^2) & -\frac{\Delta}{\rho_* F} - \frac{im}{\tau} \\ \frac{\Delta}{\rho_* F} - \frac{im}{\tau} & -\frac{E}{\rho_* F}(1-\tau^2) \end{pmatrix} \vec{g}_m. \tag{45}$$

The system (45) of two first-order coupled equations cannot be solved exactly in analytical terms. The equations contain three independent dimensionless parameters:

$$m, \quad \frac{E}{\rho_* F} = \frac{p_0 E}{\hbar F}, \quad \frac{\Delta}{\rho_* F} = \frac{p_0 \Delta}{\hbar F}. \tag{46}$$

Approximate asymptotical solutions can be obtained, which depend on the relations between these dimensionless parameters. Below, we consider the following parametric limit of Eq. (45)

$$\frac{p_0 E}{\hbar F} = \epsilon^2 \to \infty \tag{47a}$$

$$\frac{m}{\epsilon} = \sqrt{\nu} \sim 1 \tag{47b}$$

$$\frac{p_0 \Delta}{\epsilon \hbar F} = \delta \sim 1. \tag{47c}$$

The relations (47a) and (47b) define the so-called Landau-Zener limit case[17]. Relation (47c) implies $\Delta \sim E^{1/4}$ and accounts for the nontrivial role of the SO splitting Δ in the asymptotical solution. Using (47 a-c), Eq. (45) becomes:

$$-\frac{1}{2}\frac{\mathrm{d}\vec{g}}{\mathrm{d}\tau} = \left[i\epsilon^2(1-\tau^2)\hat{\sigma}_z + \frac{\epsilon\sqrt{\nu}}{\tau}\hat{\sigma}_x + \epsilon\delta\hat{\sigma}_y \right] \vec{g}.$$

$$(\epsilon \to \infty,\ \nu \sim 1,\ \delta \sim 1) \tag{48}$$

The system (48) represents a so-called singularly perturbed equation[18,19].

5. ASYMPTOTICAL SOLUTION OF THE DYNAMICAL EQUATION

We apply the matched asymptotic expansion method[18,19] for the construction of the asymptotic solution of the dynamical equation (48). The outer asymptotic expansion is a generalization of the QC approximation[20].

Let us try to construct an outer asymptotic expansion of the solution in the following way:

$$\vec{g}(\tau) \simeq (\vec{V}_0 + \frac{1}{\epsilon}\vec{V}_1 + \frac{1}{\epsilon^2}\vec{V}_2 \cdots) e^{\epsilon^2 S_2 + \epsilon S_1} \tag{49}$$

where $\vec{V}_0, \vec{V}_1, \vec{V}_2 \cdots$ and S_1, S_2 are functions of τ. The substitution of (49) into (48) and comparison of different terms of the same power of ϵ on the left-hand and right-hand sides of (48) lead to a set

of equations for $S_2, S_1, \vec{V}_0, \vec{V}_1, \vec{V}_2, \cdots$. These equations can be solved without difficulties, leading to the one-term outer asymptotic expansion ("one term" means that only the $\vec{V}_0(\tau)$ term is taken into account; the contributions of $\vec{V}_1, \vec{V}_2 \cdots$ are neglected.)

$$\begin{aligned} \vec{g}_{\text{out}}(\tau) &= C_1^+ \vec{e}_1 \left(\frac{\tau+1}{\tau-1}\right)^{i\mu} e^{-\frac{i\nu}{2\tau}} e^{-i\epsilon^2(\tau-\tau^3/3)} + \\ & \quad C_2^+ \vec{e}_2 \left(\frac{\tau+1}{\tau-1}\right)^{-i\mu} e^{\frac{i\nu}{2\tau}} e^{i\epsilon^2(\tau-\tau^3/3)} \quad \text{for } \tau > 1 \qquad (50a) \\ \vec{g}_{\text{out}}(\tau) &= C_1^- \vec{e}_1 \left(\frac{1+\tau}{1-\tau}\right)^{i\mu} e^{-\frac{i\nu}{2\tau}} e^{-i\epsilon^2(\tau-\tau^3/3)} + \\ & \quad C_2^- \vec{e}_2 \left(\frac{1+\tau}{1-\tau}\right)^{-i\mu} e^{\frac{i\nu}{2\tau}} e^{i\epsilon^2(\tau-\tau^3/3)} \quad \text{for } 0 < \tau < 1 \qquad (50b) \end{aligned}$$

where $\mu = (\nu + \delta^2)/4$ and $C_1^{\pm}, C_2^{\pm}$ are constants. This outer asymptotic expansion contains fast oscillating exponential factors and slowly varying prefactors. The solutions (50) are not valid in the so-called inner domains, near $\tau = \pm 1$ (only $\tau = 1$ is relevant for the present analysis). These inner domains are generalizations of the turning points of the QC approximation. In the inner domains, inner asymptotic expansions must be constructed (the solutions of the ethalon equations) and the outer and inner asymptotic expansions must then be matched along the anti-Stoke lines[19,21], where both fundamental solutions in the outer asymptotic expansion have purely oscillating fast exponentials (along other lines in the complex τ plane, the fast exponential factors exhibit increasing or decreasing behavior). This concept for the construction of asymptotical solutions of equations which do not admit exact analytical solutions is known as matched asymptotic expansions method in singular perturbation theory[18].

It now becomes clear why we have introduced two pairs of constants: $C_{1,2}^+$ for $\tau > 1$ and $C_{1,2}^-$ for $\tau < 1$. It is required by the different results of asymptotic matching of inner and outer solutions on the left-hand and right-hand sides of the point $\tau = 1$. In contrast to the anti-Stoke lines,

the Stoke lines correspond to purely increasing and decreasing behavior of the fast exponential factors. If a Stoke line exists between two asymptotic matchings, we expect the Stoke phenomenon in the solutions of the differential equations. It is the mathematical foundation of the theory of nonadiabatic transitions.

Analyzing the fast exponential factors in (50) in the complex τ-plane ($\tau = \tau_r + i\tau_i$) we find equations for anti-Stoke lines,

$$\tau_i \left[1 - \frac{1}{3}(3\tau_r^2 - \tau_i^2)\right] = 0 \tag{51}$$

and Stoke lines:

$$\tau_r \left[1 - \frac{1}{3}(\tau_r^2 - 3\tau_i^2)\right] = \pm 2/3. \tag{52}$$

They cross at the singular points $\tau = \pm 1$, as shown in Fig. 2. It becomes evident from Fig. 2 and from the integration path in the inverse Fourier transformation (40) that the asymptotic matching of the inner (ethalon) solution near $\tau = \pm 1$ and the outer solution (46) must be performed along the anti-Stoke lines

$$\tau_i = 0, \quad 0 < \tau_r < 1, \quad \text{and } 1 < \tau_r < \infty. \tag{53}$$

Between these two directions of asymptotic matching (left and right from $\tau = 1$) we can see Stoke lines and therefore expect the Stoke phenomenon in the solutions. The latter corresponds to a nonadiabatic effect. Note that the outer asymptotic solution (50) is in agreement with the form (37), required by Eq. (34): $\alpha = 0$, $\chi_{11} = -\chi_{22}$, and δ_0 is arbitrary.

Let us now consider the inner domain, centered at $\tau = 1$. Following general recommendations of the matched asymptotic expansions method[18], we introduce a new variable t:

$$t = \frac{\tau - 1}{\omega(\epsilon)}, \quad \tau = 1 + \omega(\epsilon)t$$

$$\omega(\epsilon) \to 0 \quad \text{when } \epsilon \to \infty. \tag{54}$$

The inner domain is characterized by $|\tau| \ll 1$, $|t| \sim 1$. In terms of the inner independent variable t, the dynamical equation (48) takes the form:

$$-\frac{1}{2}\frac{\mathrm{d}\vec{g}}{\mathrm{d}t} = \left[-i\epsilon^2\omega^2 t(2+\omega t)\hat{\sigma}_z + \epsilon\omega\sqrt{\nu}(1-\omega t+\omega^2 t^2-\cdots)\hat{\sigma}_x + \epsilon\omega\delta\hat{\sigma}_y\right]\vec{g}. \tag{55}$$

The scale $\omega(\epsilon)$ of the inner domain must be chosen such that Eq. (55) has minimal degeneracy. In other words, a maximum number of terms on the right-hand side of (55) must be of the same (main) order of magnitude (of the order of unity; this is the so-called principle of minimal degeneracy of the equation). This principle provides the best possibilities for asymptotic matching. Asymptotic matching may be carried out when the applicability domains of the outer and inner expansions are overlapping[18]. We can obey the minimal degeneracy principle in (55) by choosing

$$\epsilon\omega(\epsilon) = 1 \quad \omega(\epsilon) = 1/\epsilon$$

$$t = \epsilon(\tau - 1) \quad \tau = 1 + t/\epsilon \tag{56}$$

$$-\frac{1}{2}\frac{\mathrm{d}\vec{g}}{\mathrm{d}t} = \left[-it(2+t/\epsilon)\hat{\sigma}_z + \sqrt{\nu}(1-t/\epsilon+\cdots)\hat{\sigma}_x + \delta\hat{\sigma}_y\right]\vec{g}. \tag{57}$$

The inner asymptotic expansion can be constructed in the form of the asymptotic series

$$\vec{g}(t) \simeq \vec{g}_0(t) + \frac{1}{\epsilon}\vec{g}_1(t) + \frac{1}{\epsilon^2}\vec{g}_2(t) + \cdots \tag{58}$$

In the one-term inner asymptotic expansion, we take into account only $\vec{g}_0(t)$, neglecting the other small contributions. In this approximation, Eq. (57) becomes

$$-\frac{1}{2}\frac{\mathrm{d}\vec{g}_0}{\mathrm{d}t} = \left[-2it\hat{\sigma}_z + \sqrt{\nu}\hat{\sigma}_x + \delta\hat{\sigma}_y\right]\vec{g}_0. \tag{59}$$

An exact solution of Eq. (59) can be obtained by the method of ordered exponential operators[17,22]. In this way, we obtain (after relatively long calculations):

$$\vec{g}_0(t) = A_1\vec{A}_I(t) + A_2\vec{A}_{II}(t) \tag{60}$$

where the fundamental solutions $\vec{A}_I(t)$ and $\vec{A}_{II}(t)$ have the form

$$\begin{aligned} \vec{A}_I(t) &= \vec{e}_1 e^{\epsilon_0} - i\vec{e}_2\epsilon_+ e^{-\epsilon_0} \\ \vec{A}_{II}(t) &= -i\vec{e}_1\epsilon_- e^{\epsilon_0} + \vec{e}_2 e^{-\epsilon_0}(1-\epsilon_+\epsilon_-) \end{aligned} \tag{61}$$

where

$$\begin{aligned} \epsilon_0(t) &= \ln D_{-i\mu}(kt) \\ \epsilon_-(t) &= -(1/2\sqrt{2\pi})(\delta + i\sqrt{\nu})e^{i\pi/4}\Gamma(i\mu)D_{-i\mu}(-kt)/D_{-i\mu}(kt) \\ \epsilon_+(t) &= \left[-2\mu e^{i\pi/4}/(\delta + i\sqrt{\nu})\right] D_{-i\mu}(kt)D_{-1-i\mu}(kt) \end{aligned} \tag{62}$$

and

$$\mu = (\nu + \delta^2)/4; \qquad k = 2e^{-i\pi/4}. \tag{63}$$

$D_{i\mu}(kt)$ is the parabolic cylinder function and $\Gamma(i\mu)$ is the Gamma function[16,23]. To finish our construction of asymptotic solutions of Eq. (48), we have to perform the asymptotic matching of the inner (ethalon) solution (60)-(63) with the outer solutions (50). To achieve this, we need to take the asymptotic expressions of $\vec{g}_0(t)$ for $t \to \pm\infty$ and, at the same time, simplify (50) near $\tau = 1$. In addition, we rewrite the outer solutions in terms of the inner variable t. The asymptotic matching then results in the following relations among constant coefficients:

$$\begin{pmatrix} A_1 \\ A_2 \end{pmatrix} = \hat{H}_+ \begin{pmatrix} C_1^+ \\ C_2^+ \end{pmatrix} = \hat{H}_- \begin{pmatrix} C_1^- \\ C_2^- \end{pmatrix} \tag{64}$$

$$\begin{pmatrix} C_1^+ \\ C_2^+ \end{pmatrix} = \hat{H}_0 \begin{pmatrix} C_1^- \\ C_2^- \end{pmatrix}. \tag{65}$$

The 2×2 matrices $\hat{H}_0$, $\hat{H}_\pm$ are given in the appendix. Note that Eq. (65) is in accordance with relation (37), as it should be.

6. TRANSFORMATION TO THE COORDINATE REPRESENTATION

The inverse transformation $\vec{g}_m(k) \to \vec{\psi}_m^{(a)}(\rho)$, defined by Eq. (43), gives the radial amplitude $\vec{\psi}_m^{(a)}(\rho)$ in the coordinate representation. The integration over $\tau = \rho_* k$ extends from $\tau = 0$ to $\tau = \infty$. As we want to calculate the S-matrix for nonadiabatic transitions, the distances $\bar{\rho} = \rho/\rho_*$ must be of the order of several inner turning points:

$$\bar{\rho} \geq \bar{\rho}_{\text{in}} = m = \epsilon\sqrt{\nu} \gg 1,$$

corresponding to the classically allowed domain of motion. This implies that the Bessel functions in the matrix $\hat{N}_m^+(k, \rho)$ have large orders as well as large arguments. In this case, we can use the QC asymptotic form of the Bessel function[24,25]:

$$J_\lambda(z) \approx \sqrt{\frac{2}{\pi z}} \left(1 - \frac{\lambda^2}{z^2}\right)^{-1/4} \cos\left(\int_\lambda^z \sqrt{1 - \frac{\lambda^2}{\xi^2}}\, \mathrm{d}\xi - \frac{\pi}{4}\right).$$
$$|z| \geq |\lambda| \gg 1 \tag{66}$$

In the case under consideration, $\lambda = m \pm \frac{1}{2} \gg 1$ and $z = k\rho = \tau\bar{\rho} \gg 1$, if $\tau \sim 1$. Note that under the mentioned asymptotic conditions, the Bessel functions are rapidly oscillating functions of τ. The nonvanishing contributions to the integrals of the inverse transformation arise from the points of stationary phase. This method of evaluation of integrals with rapidly oscillating integrands is known as the stationary-phase method[26,27]. The oscillating parts of the integrands in Eq. (43c)

are given by the exponentials:

$$\exp\left[\pm i\int_{m\pm1/2}^{\tau\bar{\rho}}\sqrt{1-\frac{(m\pm1/2)^2}{\xi^2}}\,\mathrm{d}\xi\mp i\epsilon^2(\tau-\tau^3/3)\right]=\exp\left[i\phi(\lambda_1,\lambda_2,\lambda_3)\right] \tag{67}$$

where $\lambda_1,\lambda_2,\lambda_3=\pm1$.

All combinations of signs on Eq. (67) are independent; Eq. (67) thus contains eight types of rapidly oscillating factors. The stationary-phase points τ_k are determined by the equation

$$\frac{\mathrm{d}\phi}{\mathrm{d}\tau}=\pm\sqrt{\bar{\rho}^2-\frac{(m\pm1/2)^2}{\tau^2}}\mp\epsilon^2(1-\tau^2)=0$$

which is equivalent to:

$$\bar{\rho}^2-\frac{(m\pm1/2)^2}{\tau^2}=\epsilon^4(1-\tau^2)^2. \tag{68}$$

Equation (68) is a cubic equation for τ^2. There are two stationary points, $\tau_1(\bar{\rho})$ and $\tau_2(\bar{\rho})$, which give contributions to the integral. Below, we do not distinguish between $m+1/2$ and $m-1/2$ in the determination of the stationary phase points $\tau_{1,2}(\bar{\rho})$, that is, we substitute $m\pm1/2\to m$ in Eq. (68). This is a good approximation, since $m\gg1$.

The integral transformation $\vec{g}_m(k)\to\vec{\psi}_m^{(a)}(\rho)$ according to Eq. (43) includes many terms. In each term, the contribution to the integral (for fixed $\bar{\rho}$) arises from τ_1 or from τ_2, depending on the combination of signs in the oscillating factors (67). These contributions are of the type

$$\bar{\delta}=\int_0^\infty\mathcal{M}(\tau)e^{i\phi}\,\mathrm{d}\tau \tag{69}$$

where $\mathcal{M}(\tau)$ is a slowly varying function and $\exp(i\phi)$ is the rapidly oscillating factor. In the vicinity of a stationary-phase point we expand

$$\begin{aligned}\exp(i\phi)&\simeq\exp\left[i\phi(\tau_k)+(i/2)\phi''(\tau_k)(\tau-\tau_k)^2\right]\\&=\exp\left[i\phi(\tau_k)\pm(i/2)|\phi''(\tau_k)|(\tau-\tau_k)^2\right]\end{aligned} \tag{70}$$

where we have $k = 1$ or $2, \phi'(\tau_k) = 0$, $\phi''(\tau_k) = \pm|\phi''(\tau_k)|$ are real numbers and $|\phi''(\tau_k)| \gg 1$. The expression for $\bar{\delta}$, given by Eq. (69), becomes

$$\begin{aligned} \bar{\delta} &\approx \mathcal{M}(\tau_k) e^{i\phi(\tau_k)} \int_0^\infty \exp\left[\pm\frac{i}{2}|\phi''(\tau_k)|(\tau-\tau_k)^2\right] \mathrm{d}\tau \\ &= \left(\frac{2\pi}{|\phi''(\tau_k)|}\right)^{1/2} \mathcal{M}(\tau_k) e^{i\phi(\tau_k)\pm i\pi/4} \quad (k = 1 \text{ or } 2). \end{aligned} \tag{71}$$

After somewhat lengthy calculations, taking into account the contributions of all stationary-phase points, we obtain ($m \ll \bar{\rho} \ll \epsilon^2$):

$$\begin{aligned} \vec{\psi}_m^{(a)}(\bar{\rho}) \approx\ & C_1^- e^{-i\chi/2}\ \vec{\psi}_{\text{out}}^{(1)} + iC_2^- e^{i\chi/2}\ \vec{\psi}_{\text{in}}^{(1)} + \\ & C_1^+ e^{-i\chi/2}\ \vec{\psi}_{\text{in}}^{(2)} + iC_2^+ e^{i\chi/2}\ \vec{\psi}_{\text{out}}^{(2)} \end{aligned} \tag{72}$$

where

$$\begin{aligned} \vec{\psi}_{\text{in}}^{(1)} &= \exp\left[(i\zeta/2) + i\mu\ln(\bar{\rho}/\epsilon) - i\bar{\rho} + im\pi/2\right]\vec{e}_1 \\ \vec{\psi}_{\text{in}}^{(2)} &= \exp\left[(-i\zeta/2) - i\mu\ln(\bar{\rho}/\epsilon) - i\bar{\rho} + im\pi/2\right]\vec{e}_2 \end{aligned} \tag{73}$$

are incoming waves,

$$\begin{aligned} \vec{\psi}_{\text{out}}^{(1)} &= \exp\left[(-i\zeta/2) - i\mu\ln(\bar{\rho}/\epsilon) + i\bar{\rho} - im\pi/2\right]\vec{e}_1 \\ \vec{\psi}_{\text{out}}^{(2)} &= \exp\left[(i\zeta/2) + i\mu\ln(\bar{\rho}/\epsilon) + i\bar{\rho} - im\pi/2\right]\vec{e}_2 \end{aligned} \tag{74}$$

are outgoing waves and

$$\chi = \nu + (4/3)\epsilon^2 - 2\mu\ln 4\epsilon - \mu + \mu\ln\mu - \arg\left(1 + i\delta/\sqrt{\nu}\right)$$

$$\zeta = \mu - \mu\ln\mu + \arg\left(1 + i\delta/\sqrt{\nu}\right). \tag{75}$$

The asymptotic solution (72) is completed by the relation (65), which connects $C_{1,2}^+$ and $C_{1,2}^-$. These results allow us to calculate the local S-matrix for nonadiabatic transitions.

7. THE S-MATRIX FOR NONADIABATIC TRANSITIONS

We assume that the quadratic term in the JT-SO Hamiltonian (1) (which is necessary for quantization) does not significantly influence the nonadiabatic part of the problem. The nonadiabatic local S-matrix can thus be calculated in the linear-vibronic coupling approximation, that is, the Hamiltonian (2). The S-matrix calculated in this way is used (near the inner turning points) as "inner" boundary condition in the quantization problem, while the "outer" boundary condition (used near outer turning points) guarantees decreasing behavior of wave amplitudes in under-barrier domains when ρ tends to infinity. A similar method was used in Ref. 28 for the quantization in the Σ-Π-Σ four-state dynamical problem. Below, we discuss the conditions of applicability of this approximation.

According to definition, the S-matrix gives the amplitudes of the outgoing waves, acting on the amplitudes of the incoming waves. This S-matrix applies for distances $\bar{\rho}_{\rm in} = m \le \bar{\rho} \ll \epsilon^2$, which are much closer to the inner turning points than to the outer turning points. Using Eq. (72), we write:

$$\begin{pmatrix} C_1^- e^{-i\chi/2} \\ iC_2^+ e^{i\chi/2} \end{pmatrix} = \hat{S}_{\rm qc} \begin{pmatrix} iC_2^- e^{i\chi/2} \\ C_1^+ e^{-i\chi/2} \end{pmatrix} \tag{76}$$

We now use the coupling relation (65) and express the coefficients $C_{1,2}^+$ in terms of the coefficients $C_{1,2}^-$:

$$\begin{pmatrix} C_1^- e^{-i\chi/2} \\ ie^{i\chi/2}\left(e^{\pi\mu}\sqrt{1-e^{-2\pi\mu}}e^{-i\eta}C_1^- + e^{\pi\mu}C_2^-\right) \end{pmatrix} = \hat{S}_{\rm qc} \begin{pmatrix} iC_2^- e^{i\chi/2} \\ e^{-i\chi/2}\left(e^{\pi\mu}C_1^- + e^{\pi\mu}\sqrt{1-e^{-2\pi\mu}}e^{i\eta}C_2^-\right) \end{pmatrix} \tag{77}$$

The phase η is given in the appendix.

The relation (77) must be identically fulfilled for arbitrary C_1^- and C_2^-. $\hat{S}_{\rm qc}$ should be unitary and symmetrical. These requirements allow us to determine the QC S-matrix in the following form:

$$\hat{S}_{\rm qc} = -\begin{pmatrix} i\sqrt{1-e^{-2\pi\mu}}e^{i(\eta-\chi)} & e^{-\pi\mu} \\ e^{-\pi\mu} & i\sqrt{1-e^{-2\pi\mu}}e^{-i(\eta-\chi)} \end{pmatrix} \tag{78}$$

where

$$\eta - \chi = \arg\Gamma(i\mu) + \mu - \mu\ln\mu + \pi/4 \tag{79}$$

It follows from Eq. (78) that the nonadiabatic transition probability W is

$$W = e^{-2\pi\mu}. \tag{80}$$

It is interesting to compare the QC S-matrix $\hat{S}_{\rm qc}$, given by Eq. (78), with the semiclassical S-matrix, $\hat{S}_{\rm sc}$, obtained in[29]. Note that $\hat{S}_{\rm qc}$, obtained from time-independent quantum dynamical equations, is destinated for the quantum treatment of vibronic energy levels or resonances, while $\hat{S}_{\rm sc}$, obtained from the time-dependent semiclassical equations, is suitable for trajectory surface-hopping studies. The difference between $\hat{S}_{\rm qc}$ and $\hat{S}_{\rm sc}$ is in the phases of the diagonal elements. Being obtained for a specific parametric limit, the matrix $\hat{S}_{\rm qc}$ contains only one parameter $\mu \sim 1$, while $\hat{S}_{\rm sc}$ depends on two parameters (ν and σ in the notations of Ref. 29).

8. QUANTIZATION OF THE $E \times E$ JT PROBLEM WITH SO COUPLING

We consider here the linear $E \times E$ JT Hamiltonian (1) with SO coupling[1–3]. Omitting pure quantum terms, we can write the adiabatic radial potentials of the Hamiltonian (1) in the form:

$$\bar{U}_\rho^\pm = \frac{m^2\hbar^2}{2M\rho^2} \pm \sqrt{\rho^2F^2 + \Delta^2} + \frac{M\omega^2\rho^2}{2}. \tag{81}$$

Let us introduce inner and outer turning points, which define the domain of classically allowed motion:

$$\rho_{\rm in}^{(1)} \approx \rho_{\rm in}^{(2)} \approx m\rho_* \tag{82}$$

$$\rho_{\rm out}^{(1,2)} \approx \frac{F}{M\omega^2}\left(\sqrt{\frac{\omega^2 p_0^2}{F^2}+1} \mp 1\right). \tag{83}$$

We also need the left-counted ($S_{1,2}$), right-counted ($\phi_{1,2}$), and complete action integrals ($\Omega_{1,2}$):

$$S_{1,2} = \int_{\rho_{\rm in}}^{\rho} \sqrt{2M(E-\bar{U}_\rho^{\pm})}\ {\rm d}\rho \tag{84}$$

$$\phi_{1,2} = \int_{\rho_{\rm out}^{(1,2)}}^{\rho} \sqrt{2M(E-\bar{U}_\rho^{\pm})}\ {\rm d}\rho \tag{85}$$

$$\Omega_{1,2} = \int_{\rho_{\rm in}}^{\rho_{\rm out}^{(1,2)}} \sqrt{2M(E-\bar{U}_\rho^{\pm})}\ {\rm d}\rho. \tag{86}$$

When ρ belongs to the classically allowed domain ($\rho_{\rm in} < \rho < \rho_{\rm out}^{1,2}$), we can write the QC solutions for $\vec{\psi}_m^{(a)}(\rho)$ in the following form

$$\begin{aligned}\vec{\psi}_m^{(a)}(\rho) &= \frac{B_1^+\vec{e}_1}{\sqrt{P_1(\rho)}}e^{\frac{i}{\hbar}S_1} + \frac{B_1^-\vec{e}_1}{\sqrt{P_1(\rho)}}e^{-\frac{i}{\hbar}S_1} \\ &\quad + \frac{B_2^+\vec{e}_2}{\sqrt{P_2(\rho)}}e^{\frac{i}{\hbar}S_2} + \frac{B_2^-\vec{e}_2}{\sqrt{P_2(\rho)}}e^{-\frac{i}{\hbar}S_2} \qquad (87)\\ &= \frac{D_1^+\vec{e}_1}{\sqrt{P_1(\rho)}}e^{\frac{i}{\hbar}\phi_1} + \frac{D_1^-\vec{e}_1}{\sqrt{P_1(\rho)}}e^{-\frac{i}{\hbar}\phi_1} \\ &\quad + \frac{D_2^+\vec{e}_2}{\sqrt{P_2(\rho)}}e^{\frac{i}{\hbar}\phi_2} + \frac{D_2^-\vec{e}_2}{\sqrt{P_2(\rho)}}e^{-\frac{i}{\hbar}\phi_2} \qquad (88)\end{aligned}$$

where

$$P_{1,2}(\rho) = \sqrt{2M(E-\bar{U}_\rho^{\pm})}. \tag{89}$$

The QC solution (88) is exponentially decreasing for $\rho > \rho_{\rm out}^{1,2}$, if for $\rho < \rho_{\rm out}^{1,2}$ it has the form[30]:

$$\begin{aligned}\vec{\psi}_m^{(a)}(\rho) &= \frac{D_1^+\vec{e}_1}{\sqrt{P_1(\rho)}}\cos\left(\frac{1}{\hbar}\phi_1(\rho)+\frac{\pi}{4}\right) \\ &\quad + \frac{D_2^+\vec{e}_2}{\sqrt{P_2(\rho)}}\cos\left(\frac{1}{\hbar}\phi_2(\rho)+\frac{\pi}{4}\right).\end{aligned} \tag{90}$$

It follows from (90) that

$$\begin{pmatrix} D_1^+ \\ D_2^+ \end{pmatrix} = i \begin{pmatrix} D_1^- \\ D_2^- \end{pmatrix}. \tag{91}$$

The relations (84)-(88) lead to the following couplings between coefficients

$$\begin{pmatrix} D_1^+ \\ D_2^+ \end{pmatrix} = \begin{pmatrix} e^{i\Omega_1/\hbar} & 0 \\ 0 & e^{i\Omega_2/\hbar} \end{pmatrix} \begin{pmatrix} B_1^+ \\ B_2^+ \end{pmatrix}$$
$$\begin{pmatrix} D_1^- \\ D_2^- \end{pmatrix} = \begin{pmatrix} e^{-i\Omega_1/\hbar} & 0 \\ 0 & e^{-i\Omega_2/\hbar} \end{pmatrix} \begin{pmatrix} B_1^- \\ B_2^- \end{pmatrix}. \tag{92}$$

Taking into account relations (91) and (92), we have

$$\begin{pmatrix} B_1^+ \\ B_2^+ \end{pmatrix} = i \begin{pmatrix} e^{-2i\Omega_1/\hbar} & 0 \\ 0 & e^{-2i\Omega_2/\hbar} \end{pmatrix} \begin{pmatrix} B_1^- \\ B_2^- \end{pmatrix}. \tag{93}$$

A second relation between $B_{1,2}^+$ and $B_{1,2}^-$ is given by the nonadiabatic QC S-matrix

$$\begin{pmatrix} B_1^+ \\ B_2^+ \end{pmatrix} = \hat{S}_{\rm qc} \begin{pmatrix} B_1^- \\ B_2^- \end{pmatrix} \tag{94}$$

where $\hat{S}_{\rm qc}$ is defined by (78)-(79). The combination of (93) and (94) leads to the secular equation

$$\cos\left(\tilde{\Omega}_1 + \tilde{\Omega}_2\right) + \sqrt{1 - e^{-2\pi\mu}} \cos\left(\tilde{\Omega}_1 - \tilde{\Omega}_2\right) = 0 \tag{95}$$

$$\tilde{\Omega}_{1,2} = \Omega_{1,2}/\hbar \pm (\eta - \chi)/2. \tag{96}$$

Note that in the special case $\Delta = 0$ the secular equation (95)-(96) becomes identical to the secular equation derived in Ref. 10.

Let us consider two limiting cases: $\mu \ll 1$ and $\mu \gg 1$. In diabatic limiting case, $\mu \ll 1$, we have

$$\cos\left(\tilde{\Omega}_1 + \tilde{\Omega}_2\right) = 0, \tag{97}$$

which describes quantization in an united well. In the adiabatic limiting case, $\mu \gg 1$, we have independent quantization in two radial adiabatic potentials $\bar{U}_\rho^\pm$:

$$\cos\tilde{\Omega}_1 \cdot \cos\tilde{\Omega}_2 = 0$$

$$(\eta - \chi) \to 0 \quad \text{when} \quad \mu \to \infty. \tag{98}$$

In the adiabatic limit, there are two series of vibronic energy levels, one increasing with F, the other decreasing with increasing F. As is well known for the JT problem without SO coupling, there exist avoided crossings between both series of levels[10,13]. The energy splitting at the avoided crossing points is equal to:

$$\Delta E = (\hbar/\pi)\sqrt{\omega_1\omega_2}e^{-\pi\mu} \tag{99}$$

where

$$\omega_{1,2} = \pi\left[\int_{\rho_{\rm in}}^{\rho_{\rm out}^{(1,2)}} \frac{M\ \mathrm{d}\rho}{\sqrt{2M(E-\bar{U}_\rho^\pm)}}\right]^{-1}_{E=E_0} \tag{100}$$

are the frequencies of periodic classical motion in potentials $\bar{U}_\rho^\pm$ and E_0 is vibronic energy in the crossing point[10]. It is useful to represent relation (99) in the following form

$$\Delta E = Z(E,m,F,\Delta) \times \exp\left[-\frac{\pi}{4}\left(\frac{\hbar F m^2}{E\sqrt{2ME}} + \frac{\Delta^2\sqrt{2M/E}}{\hbar F}\right)\right], \tag{101}$$

where $Z(E,m,F,\Delta)$ is a slowly varying function of its arguments.

We need to formulate also a requirement on the quadratic term in (81). The quadratic term must be relatively small near the inner turning point. This requirement is necessary to justify the use of the nonadiabatic S-matrix, $\hat{S}_{\rm qc}$, obtained in the linear approximation. In the case under consideration the restriction

$$\omega \le \sqrt{\epsilon}F/p_0 \tag{102}$$

is sufficient to guarantee the correctness of the theory.

9. NUMERICAL CALCULATIONS OF ENERGY LEVELS

9.1. Matrix-diagonalization method

Using the spin-vibronic Hamiltonian of Eq. (1), the Schrödinger equation

$$\hat{H}_{\rm JT}\Psi_\nu = E_\nu \Psi_\nu \tag{103}$$

is solved, using an expansion of the diabatic state function Ψ_ν in a complete basis, which is constructed as the product of electronic ($|\phi_e\rangle$) and vibrational ($|nl\rangle$) basis functions[31]. The $|nl\rangle$, $n = 0, 1, 2\cdots$, $l = -n, -n+2, \cdots n-2, n$, are the eigenfunctions of the two-dimensional isotropic harmonic oscillator[32].

The real symmetric Hamiltonian matrix is constructed and diagonalized for a given value of m, which is an exact quantum number of the problem. The vibrational basis is increased until convergence of the eigenvalues of interest has been achieved. A standard diagonalization method for real symmetric matrices has been used. The eigenvalues represent the vibronic energy levels $E_\nu^{(m)}$ with vibronic angular momentum quantum number m. These calculations are very efficient since the matrix elements of the Hamiltonian are known in analytical form[31].

9.2. Quasiclassical Method

The numerical solution of the secular equation, Eq. (95), has been achieved using the following strategy. For a given set of values of m, ω, f, and Δ, the solutions of Eq. (95) are obtained by increasing E in small intervals and using the bisection method for the determination of the solution up to the desired level of accuracy. The lower boundary of the search procedure is the minimum

of the upper PES $\bar{U}_\rho^+$ of Eq. (81). For any given value of the energy, the inner and the outer turning points of both surfaces are determined numerically using the bisection method, where Eqs. (82) and (83) provide good starting guesses. The numerical integration (Eq. (86)) is performed using Simpson's rule[33]. The size of the subintervals is reduced until convergence of the integral is achieved. The Γ function, used in Eq. (79) is calculated via the following series expansion[34]:

$$\frac{1}{\Gamma(z)} = \sum_{k=1}^{\infty} c_k z_k \qquad (|z| < \infty), \tag{104}$$

The coefficients c_k $(k = 1, \cdots 26)$ are given in Ref. 34.

9.3. Comparative analysis of quasiclassical and numerically exact energy levels

In this section, we compare the vibronic energy levels obtained from two different methodologies, i.e., the matrix-diagonalization (MD) method and the QC approximation, for the $E\times E$ JT problem with SO coupling. While the MD method provides all energy levels, the energy levels lying below the minimum energy of $\bar{U}_\rho^+$ cannot be determined by the QC method. The QC approximation is known to produce the most accurate results for large vibronic angular momenta and in the high-energy limit.

Figure 3 shows the comparison of the MD and QC methods for $m = 20.5$ and $\Delta/\hbar\omega = 0$. The vibronic energy levels are plotted as a function of the JT coupling constant (F). The vibronic energy levels obtained from the MD method are shown by solid lines, while those of the QC method are shown by dotted lines in the Figs. 3, 4, 5, and 6. The agreement between the two methods is rather good for all values of F. The agreement is excellent, in particular, in the moderate JT coupling regime. For weak JT coupling, the accuracy of the QC approximation improves for high-lying vibronic energy levels, see Fig. 3.

The comparison between the QC and exact energy levels for a moderate value of $\Delta/\hbar\omega$ (= 0.8) is depicted in Fig. 4. The QC method does not describe the vibronic levels with great accuracy for weak JT coupling, but remains qualitatively correct. The reason is the violation of the limiting condition (47) for very weak JT coupling (and moderate SO coupling). For moderate and strong JT coupling, however, the agreement is excellent, even for the low-lying vibronic levels.

Having obtained a satisfactory prediction of the vibronic levels for large vibronic angular momenta, we investigate the performance of the QC approximation for low values of vibronic angular quantum number ($m = 1.5$) in Fig. 5 for $\Delta/\omega = 0$. With the exception of the strong coupling region, $F/(\hbar^{1/2}M^{1/2}\omega^{3/2}) \gg 1$, the QC method agrees very well with the MD method and this agreement gets better for high energies. For strong JT coupling and low energy levels, the QC approximation fails (due to violation of the limiting condition (47a)).

The comparison of QC and exact results for a moderate value of SO coupling, ($\Delta/\hbar\omega = 0.8$) and a small value of m (=1.5) is shown in Fig. 6. For low values of F, the QC approximation is poor, which is again the consequence of the violation of the limiting condition (47c). For larger value of F, the agreement is very good, see Fig. 6.

An additional explanation of some deviations between the QC and exact results in Figs. 4 and 6 for small F is the violation of the condition (101). Rigorously speaking, the good agreement between QC and exact results in Figs. 3 and 5 is unexpected: The relation (47c) is violated for $\Delta = 0$. To explain this finding we note that in the particular case $\Delta = 0$ our QC and exact numerical results are identical to those one obtained in Ref. 10 for the JT problem without SO coupling.

10. CONCLUSIONS

The SO interaction manifests itself in the energy splitting 2Δ of the electronic adiabatic terms at the symmetrical configuration. It modifies the symmetry properties of the radial Hamiltonian, which arises as a result of the separation of variables in the Schrödinger equation for the nuclear wave amplitudes. The corresponding symmetry operator includes a change of sign of the SO parameter Δ. The radial adiabatic potentials $U_\rho^\pm$ include new terms which arise from the SO coupling. The radial nonadiabatic dynamical coupling in the adiabatic representation (11) is of pure SO origin. There are three centers of nonadiabatic transitions

$$r_0^0 = 0, \qquad r_0^\pm = \pm i\Delta/F,$$

where nonadiabatic coupling terms become singular. The centers $r_0^\pm$ are absent in the nonrelativistic limit $\Delta = 0$.

In the linear JT coupling approximation, the momentum representation reduces the general order of the differential dynamical equations from four to two. While the continuous symmetry of the Hamiltonian in the momentum representation is identical to the continuous symmetry of the Hamiltonian in the coordinate representation, the discrete symmetries are different in these representations. The conservation law for the dynamical equations in the momentum representation is of essentially non-hermitian character. The corresponding evolution operator obeys hyperbolic unitary conditions.

The two-dimensional Fourier transformation from coordinate to momentum representation in Cartesian variables is equivalent to a matrix-integral transformation of Bessel type for the radial wave amplitudes in polar variables. In the QC Landau-Zener limit, the linear JT-SO problem

admits a complete analytical solution in terms of elementary and special functions. The latter are the Gamma function, Bessel functions, and parabolic-cylinder functions.

The linear JT-SO problem contains four dimensionless parameters (ϵ, ν, δ, $E/\hbar\omega$); only one of them (δ) is caused by the SO interaction. The nonadiabatic transitions arise as the Stoke phenomenon in the asymptotical solution of the dynamical equations. The asymptotical solution in the coordinate representation has the form of a pair of incoming and a pair of outgoing waves; these pairs are connected by the nonadiabatic 2×2 S-matrix, which is unitary and symmetrical. The nonadiabatic transition probability (given by the square of the nondiagonal element of the S-matrix) is $W = \exp(-2\pi\mu)$, where μ may be interpreted as a generalized Landau-Zener parameter.

The role of the quadratic term in Hamiltonian is to restrict the classically available domain of motion and to transform the continuous spectrum to a discrete (bound-state) spectrum. The secular equation for the vibronic energy levels includes adiabatic action integrals ($\Omega_{1,2}$), the generalized Landau-Zener parameter (μ) and a nonadiabatic phase ($\nu - \chi$). In the diabatic limit ($\mu \to 0$) we have quantization in an united potential well.

In the adiabatic limit ($\mu \to \infty$), there are two independent quantizations in the radial adiabatic potentials $\bar{U}_\rho^{\pm}$. In the near-adiabatic limit, we have avoided crossings of vibronic energy levels depending on the coupling constants F and the SO splitting Δ. These avoided crossings are due to the nonadiabatic transitions present in the system. In general, the existence of the SO splitting Δ increases the value of the Landau-Zener parameter μ, shifts the dynamical regime to the adiabatic limit, and reduces the vibronic-energy splittings in the avoided crossing points.

The numerically exact calculation of energy levels confirms in general the validity of the QC results. Limitations of the QC approximation can be observed for large and small values of the

JT coupling constant F. They arise as a consequence of the violation of the limiting relations (47) (generalized Landau-Zener limit) and the violation of condition (101) (validity of the nonadiabatic S-matrix, obtained in the linear approximation). The dependence of the characteristic avoided crossings of the vibronic energy levels on the JT coupling constant, the SO coupling constant, and the vibronic angular momentum have been analyzed in detail on the basis of the analytic expressions. From Eq. (101) it is clear that the dependence of the vibronic-energy splitting on the parameters m and Δ are essentially given by Gaussian functions.

In this work, we have been concerned with the calculation of bound vibronic energy levels, which can efficiently be calculated numerically by the diagonalization of large sparse matrices. The QC analysis is not restricted to the bound-state problem. It may be employed, for example, for the calculation of the positions and widths of resonances associated with the upper well of the purely linear $E \times E$ JT Hamiltonian with SO coupling [Eq. (2)]. The numerical calculation of these resonances requires coupled-channel scattering calculations which are considerably more involved than the numerical calculations of bound vibronic states.

The applicability of the systematic asymptotic expansion methods outlined in the present work is not restricted to the $E \times E$ JT problem. Other, more general, vibronic-coupling problems such as the pseudo-JT effect and Σ-Π coupling in linear molecules may be treated with these methods. The advantage of the analytical QC methods is that they provide explicit insight into the nature of the nonadiabatic effects in such systems which cannot be obtained from the purely numerical calculation of energy levels.

Acknowledgement

This work has been supported by the Deutsche Forschungsgemeinschaft via a research grant and a visitor grant for L.V.P.

The matrices $\hat{H}_{\pm}$, $\hat{H}_0$, resulting from asymptotic matching procedures, are

$$\hat{H}_+ = \begin{pmatrix} \exp\left(\frac{\pi\mu}{4} - \frac{i\nu}{2} - \frac{2i\epsilon^2}{3} + i\mu\ln 4\epsilon\right) & \left[(\delta + i\sqrt{\nu})\Gamma(i\mu)/(2\sqrt{2\pi})\right] \times \\ & \exp\left(-i\mu\ln 4\epsilon + \frac{i\nu}{2} + \frac{2i\epsilon^2}{3} - \frac{i\pi}{4} + \frac{3\pi\mu}{4}\right) \\ 0 & \exp\left(-i\mu\ln 4\epsilon - \frac{\pi\mu}{4} + \frac{i\nu}{2} + \frac{2i\epsilon^2}{3}\right) \end{pmatrix} \tag{.1}$$

$$\hat{H}_- = \begin{pmatrix} 0 & \left[(\delta + i\sqrt{\nu})\Gamma(i\mu)/(2\sqrt{2\pi})\right] \times \\ & \exp\left(-i\mu\ln 4\epsilon - \frac{i\pi}{4} - \frac{\pi\mu}{4} + \frac{i\nu}{2} + \frac{2i\epsilon^2}{3}\right) \\ \left[(-2\sqrt{2\pi})/\left((\delta + i\sqrt{\nu})\Gamma(i\mu)\right)\right] \times & \exp\left(-i\mu\ln 4\epsilon + \frac{i\nu}{2} + \frac{2i\epsilon^2}{3} + \frac{3\pi\mu}{4}\right) \\ \exp\left(i\mu\ln 4\epsilon + \frac{i\pi}{4} + \frac{\pi\mu}{4} - \frac{i\nu}{2} - \frac{2i\epsilon^2}{3}\right) & \end{pmatrix} \tag{.2}$$

$$\hat{H}_0 = \begin{pmatrix} e^{\pi\mu} & e^{\pi\mu}\sqrt{1 - e^{-2\pi\mu}}e^{i\eta} \\ e^{\pi\mu}\sqrt{1 - e^{-2\pi\mu}}e^{-i\eta} & e^{\pi\mu} \end{pmatrix} \tag{.3}$$

where

$$\eta = \arg\Gamma(i\mu) + \arg\left(\delta + i\sqrt{\nu}\right) - 2\mu\ln 4\epsilon + \nu - \frac{\pi}{4} + \frac{4\epsilon^2}{3}. \tag{.4}$$

---

* Corresponding author. Tel.: +49-89-289-13618; fax: +49-89-289-13622.
Email addresses: poluyan@icp.ac.ru (L. V. Poluyanov), sabyashachi.mishra@ch.tum.de (S. Mishra), domcke@ch.tum.de (W. Domcke)

[1] H. Koizumi and S. Sugano, J. Chem. Phys. **102**, 4472 (1995).
[2] J. Schön and H. Köppel, J. Chem. Phys. **108**, 1503 (1998).
[3] W. Domcke, S. Mishra, and L. V. Poluyanov, Chem. Phys. **322**, 405 (2006).
[4] A. I. Voronin and V. I. Osherov, J. Exp. Theor. Phys. **39**, 62 (1974) (In English).
[5] E. Teller, J. Phys. Chem. **41**, 109 (1937).
[6] H. A. Jahn and E. Teller, Proc. Roy. Soc. London **A161**, 220 (1937).
[7] J. Neumann and E. Wigner, Physik. Z. **30**, 467 (1929).
[8] E. Wigner, *Nachrichten Akad. Wiss. Göttingen. Math.-Phys. Kl*, Berlin, 1930.
[9] H. C. Longuet-Higgins, Proc. Roy. Soc. London **A344**, 147 (1975).
[10] A. I. Voronin, S. P. Karkach, V. I. Osherov, and V. G. Ushalov, J. Exp. Theor. Phys. **44**, 465 (1976) (In English).

[11] B. R. Judd and E. E. Vogel, Phys. Rev. B **11**, 2427 (1975).

[12] B. R. Judd, J. Chem. Phys. **68**, 5643 (1978).

[13] I. B. Bersuker, *The Jahn-Teller Effect*, Cambridge University Press, 2006.

[14] E. E. Nikitin, *Theory of Elementary Atomic and Molecular Processes in Gases*, Clarendon Press, Oxford, 1974.

[15] *Conical Intersections : Electronic Structure, Dynamics and Spectroscopy*, edited by W. Domcke, D. R. Yarkony, and H. Köppel, World Scientific, Singapore, 2004.

[16] L. S. Gradshteyn and I. M. Ryzhik, *Tables of Integrals Series and Products*, Academic Press, New York, 1994.

[17] V. I. Osherov and L. V. Poluyanov, Chem. Phys. Reports **17**, 1999 (1999).

[18] M. van Dyke, *Perturbation Methods in Fluid Mechanics*, Academic Press, New York, 1964.

[19] A. Aguilar, M. Gonzales, and L. V. Poluyanov, Mol. Phys. **72**, 193 (1992).

[20] A. H. Nayfen, *Perturbation Methods*, Wiley, New York, 1973.

[21] P. V. Elyutin and V. D. Krivchenkov, *Quantum Mechanics*, Nauka, Moscow (In Russian), 1976.

[22] J. Wei and E. Norman, J. Math. Phys. **4**, 575 (1963).

[23] H. Bateman and A. Erdelyi, *Higher Transcedental Functions*, Mc. Graw-Hill, New York, 1953.

[24] V. I. Osherov, V. G. Ushakov, and A. I. Voronin, J. Phys. B: Atom. Mol. Phys. **13**, 1507 (1980).

[25] L. V. Poluyanov and R. Schinke, Chem. Phys. **288**, 123 (2003).

[26] A. Erdelyi, *Asymptotic Expansions*, Dover Publications, New York, 1955.

[27] M. V. Fedoryuk, *Asymptotics, Integrals and Series*, Nauka, Moscow (In Russian), 1987.

[28] L. V. Poluyanov and W. Domcke, Chem. Phys. **293**, 179 (2003).

[29] L. V. Poluyanov and W. Domcke, Chem. Phys. **322**, 349 (2006).

[30] L. D. Landau and E. M. Lifshitz, *Quantum Mechanics*, Akademie-Verlag, Berlin, 1967.

[31] H. C. Longuet-Higgins, in *Advances in Spectroscopy*, edited by H. W. Thompson, Vol. II, p. 429, Interscience, New York, 1961.

[32] L. Schiff, *Quantum Mechanics*, McGraw-Hill, 1968.

[33] P. J. Davis and P. P. Rabinowitz, *Methods of Numerical Integration*, Academic Press, New York, 1975.

[34] M. Abramowitz and I. A. Stegun, *Handbook of Mathematical Functions*, Dover Publications, New York, 1965.

FIGURES

FIG. 1: Qualitative view of the radial adiabatic terms $U_\rho^\pm$ (solid lines) and adiabatic terms $\pm U$(dashed lines). The minimum of U_ρ^+ is $\bar{\rho} = (\hbar m)^{2/3}/(FM)^{1/3}$.

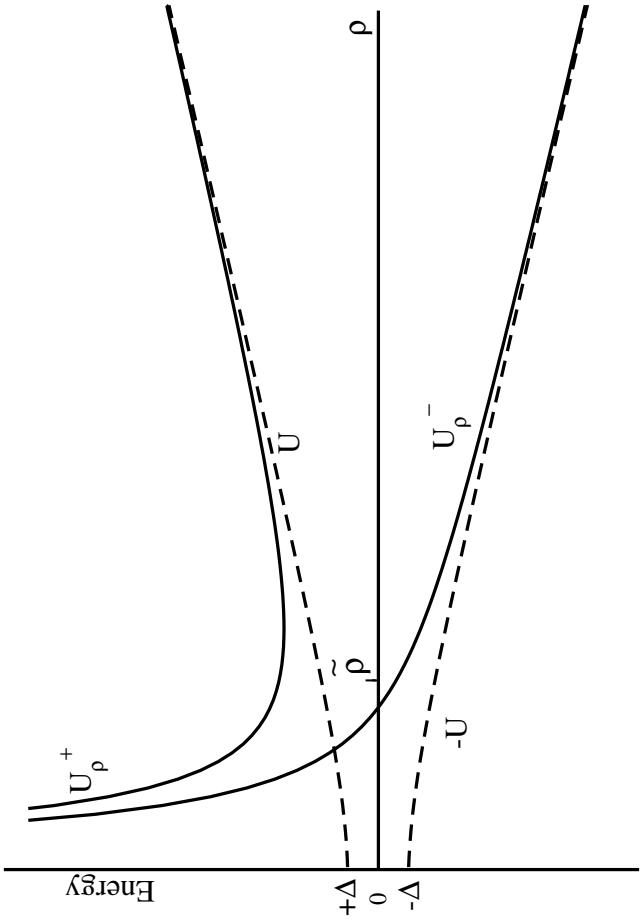

FIG. 2: Anti-Stoke lines (solid lines), Stoke lines (dashed lines), and ethalon domains (inner domains) (circles). The domains of solution (50a) and (50b) are indicated by the (+) and (-) symbols.

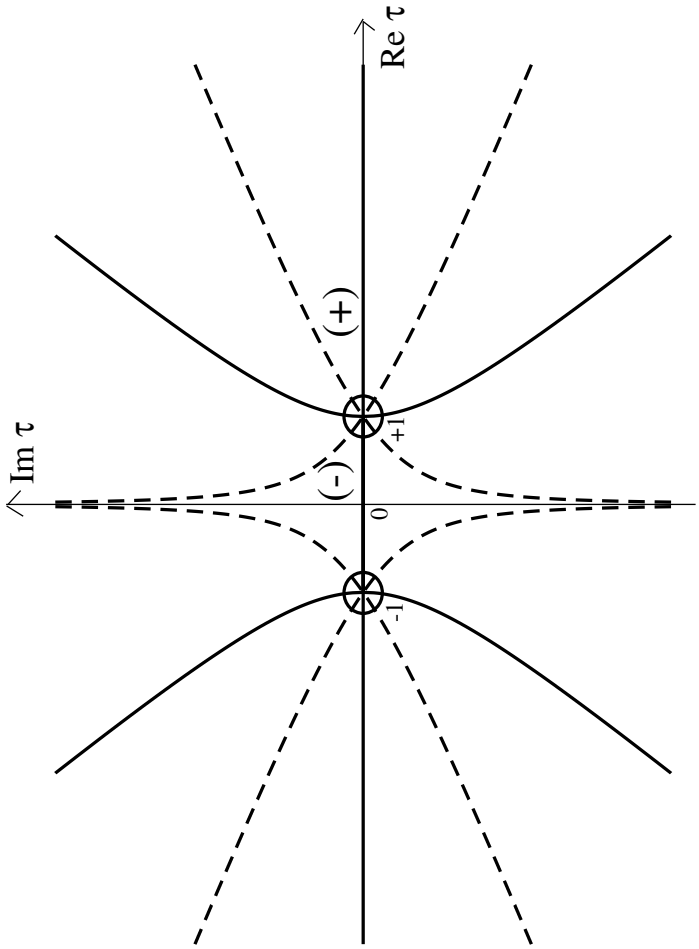

FIG. 3: Vibronic energy levels as a function of the vibronic coupling constant F, for m=20.5, $\Delta/\hbar\omega$=0; quasiclassical results are given as dotted lines, matrix diagonalization results as solid lines.

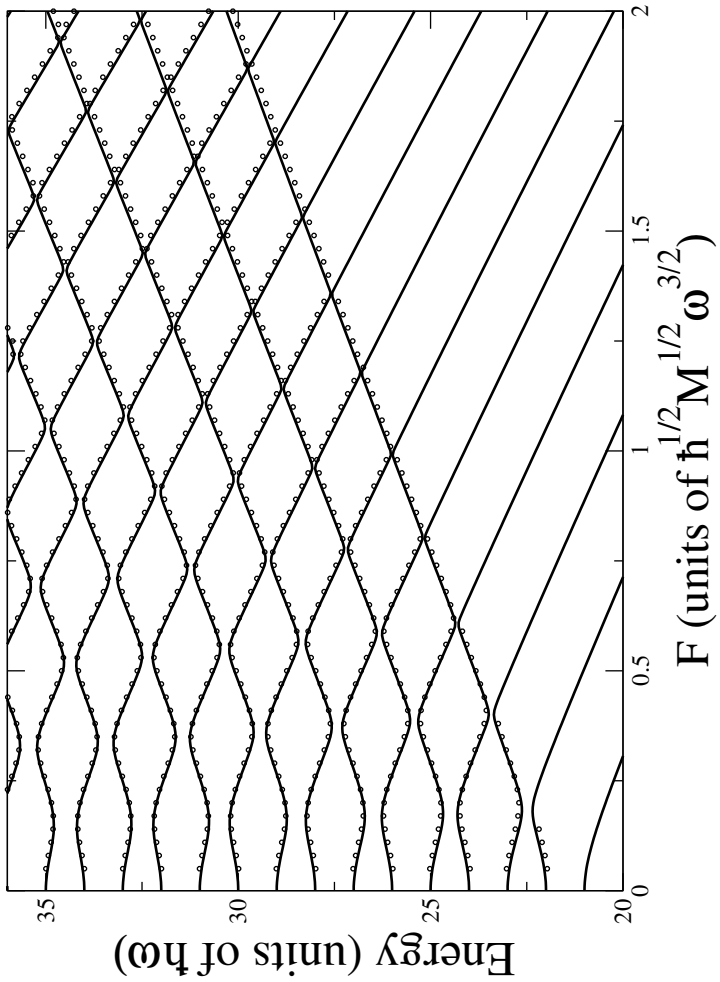

FIG. 4: Vibronic energy levels as a function of the vibronic coupling constant F, for m=20.5, $\Delta/\hbar\omega$=0.8; quasiclassical results are given as dotted lines, matrix diagonalization results as solid lines.

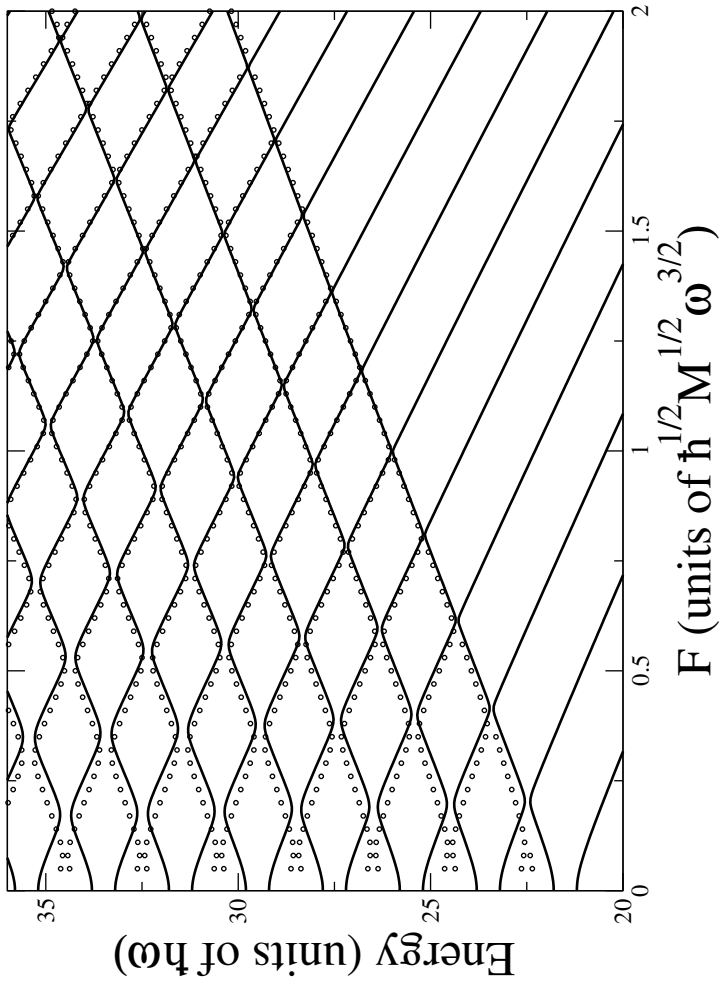

FIG. 5: Vibronic energy levels as a function of the vibronic coupling constant F, for m=1.5, $\Delta/\hbar\omega$=0; quasiclassical results are given as dotted lines, matrix diagonalization results as solid lines.

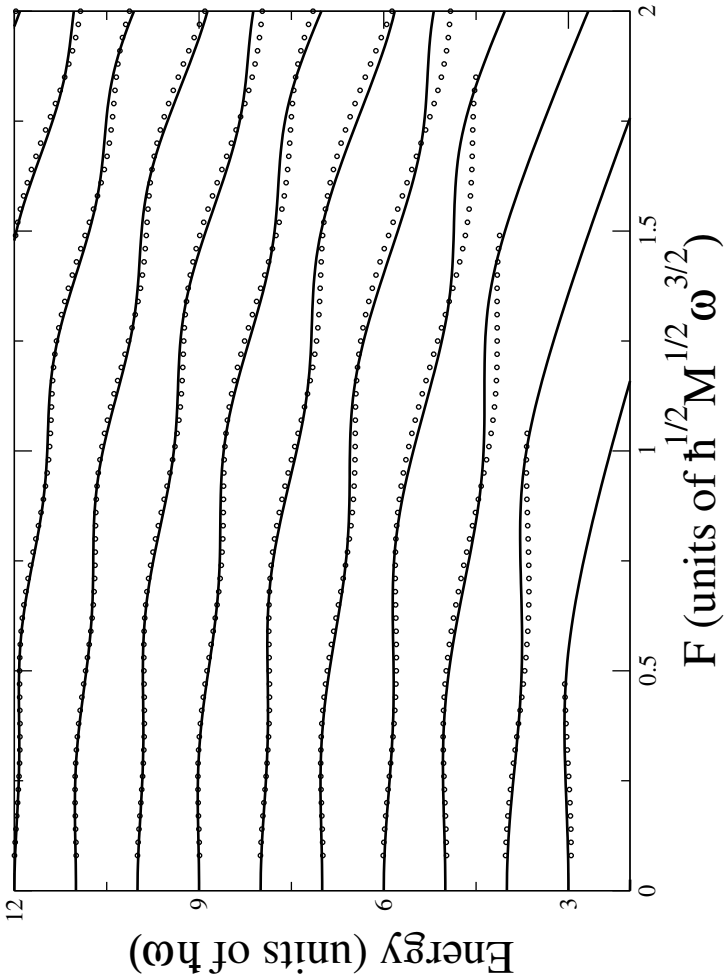

FIG. 6: Vibronic energy levels as a function of the vibronic coupling constant F, for m=1.5, $\Delta/\hbar\omega$=0.8; quasiclassical results are given as dotted lines, matrix diagonalization results as solid lines.

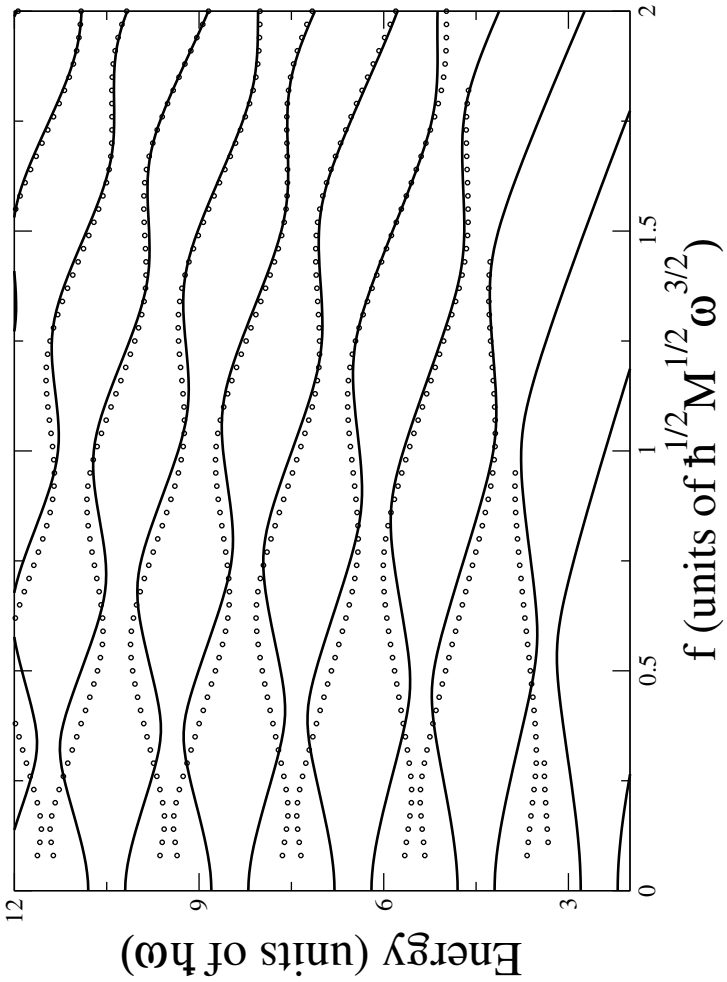

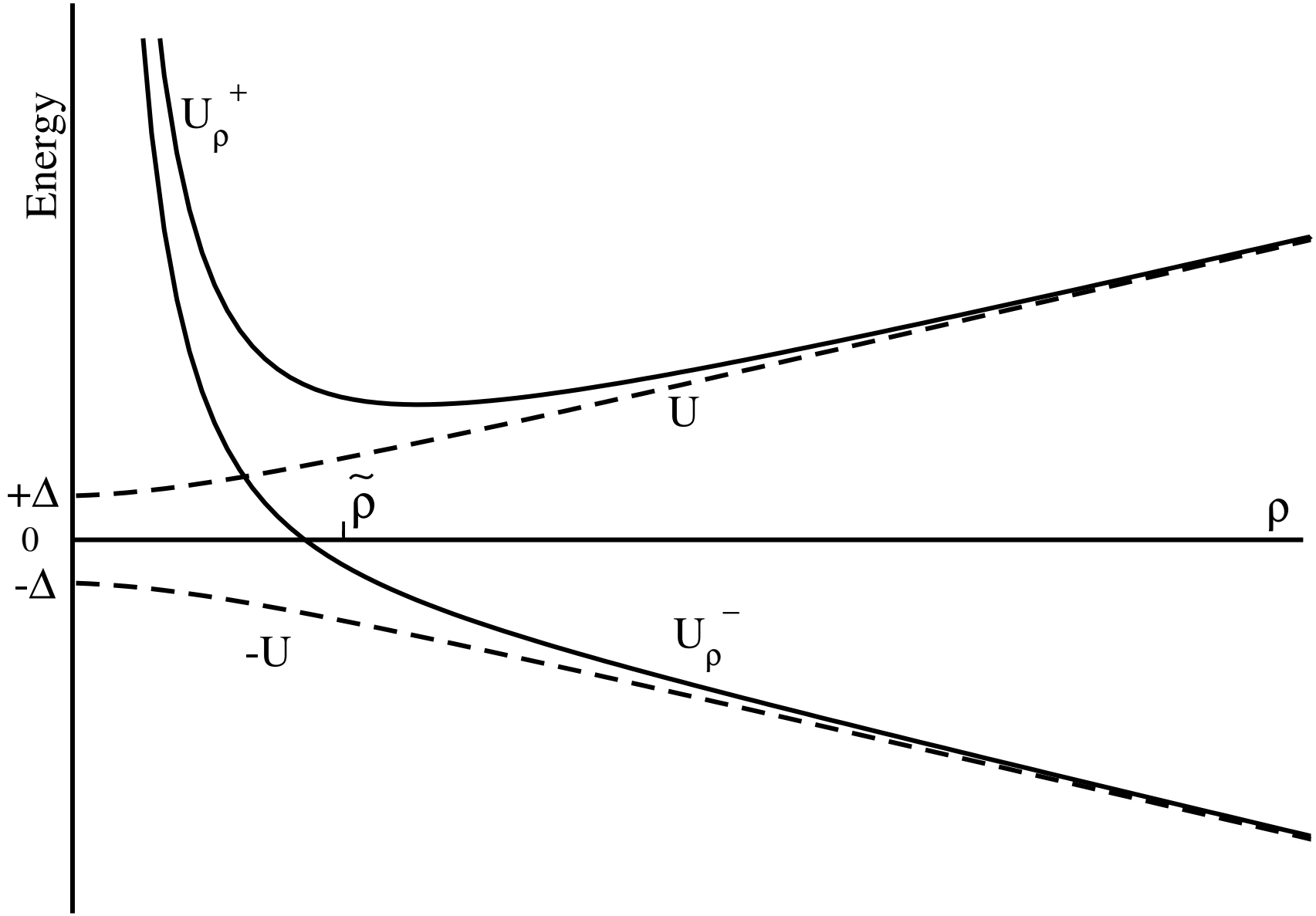
Energy
U_ρ^+
U
$+\Delta$
0
$-\Delta$
$\tilde{\rho}$
ρ
-U
U_ρ^-

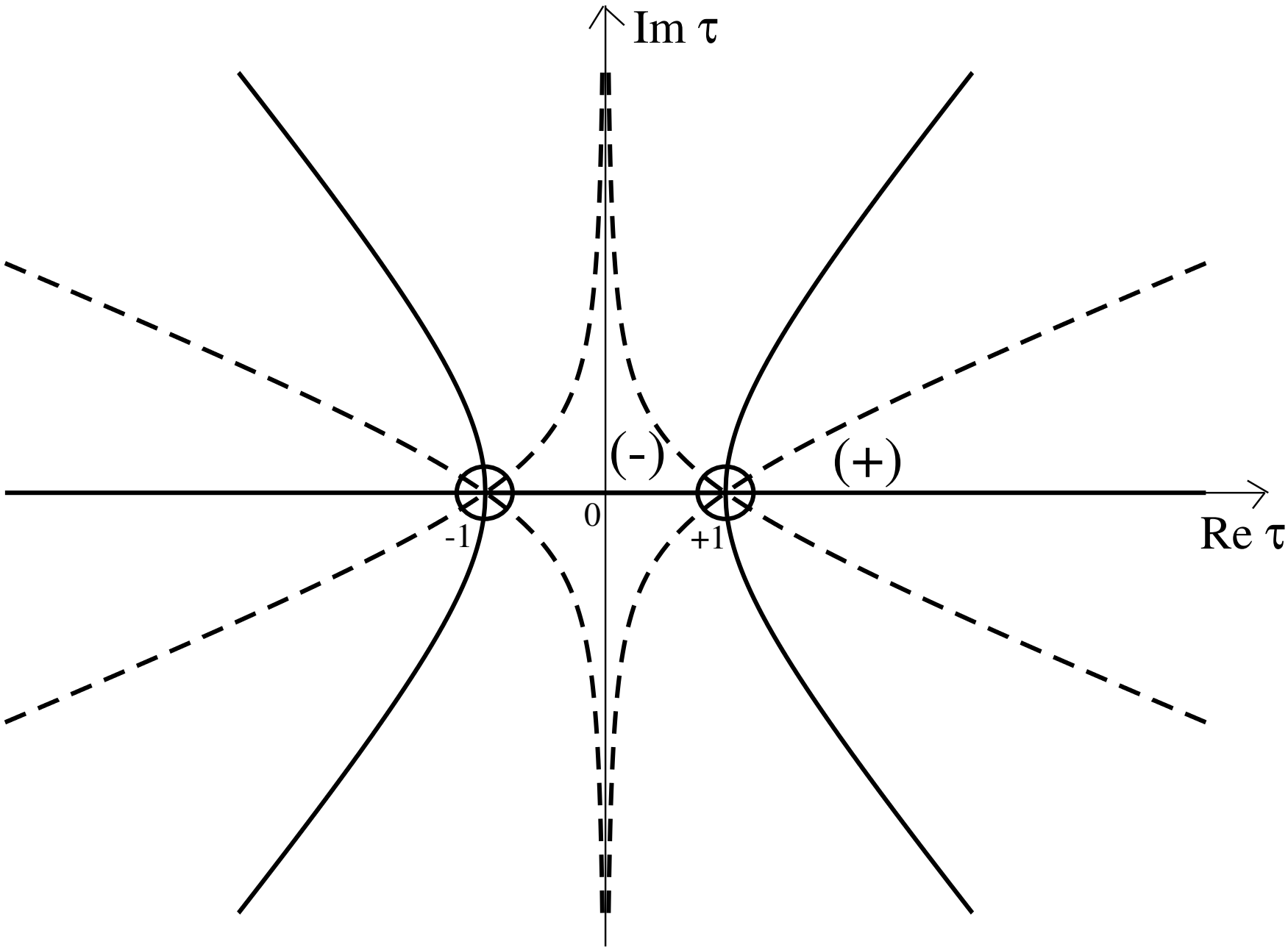
Im τ
Re τ
(-)
(+)
0
-1
+1